Evaluation of MM5 for simulating radiation and surface energy balance parameter observations at Scott Base during 25th to 31st October 2003

Catherine Tisch
GCAS 2004/5
Supervised Project
ID: 0108480

Abstract

Observations were conducted near Scott Base during 2003-2004, with the objective of measuring parameters that may give rise to processes that control meltwater production on the McMurdo Ice Shelf. Observations were then compared with simulations produced by MM5 of the same time period, of which a portion was described in detail in this report. Some parameters such as downward shortwave radiation, upward shortwave radiation, net radiation and wind direction were accurately depicted by the modelled simulations, having correlation coefficients of 0.97, 0.95, 0.89 and 0.80 respectively. Other parameters had a negative or positive bias. In this instance, the model does not capture the intensity or accuracy of the observed recordings. It is identified that climate modelling is essential for understanding the way in which planet Earth operates and that accurately modelling the current climate will help produce more powerful model and accurate models to help identify what the future climate might be like. The precise modelling of Antarctica is integral to this understanding of climate change.

Introduction

The importance of climatic modelling for understanding planet Earth

Predicting how the Earth's climate may fluctuate in response to natural and anthropogenic change is one of the greatest challenges facing scientists today. Yet the knowledge of the way in which the climate system works (in terms of its component parts and the ways in which they interact), is far from complete. It is now commonly accepted that atmospheric and oceanic processes in the Polar Regions exert strong controls on global climate, but the understanding of how, when and where remains limited. This is where the importance of climatic modelling becomes crucial. By quantifying the role of Antarctic process in controlling global climate, models will contribute to more accurate predictions of future climate change. However, before this can take place, models need to be produced and refined to accurately simulate the current climate, before accurate modelling of the past or future can take place.

Over the past decade numerical weather prediction and simulations over the Polar Regions has made significant progress. Extreme weather phenomena (such as surface air temperatures routinely below -50°C), complex atmospheric flow and sharp topographic contrasts create unique difficulties and challenges when modelling atmospheric processes Antarctica. The continual improvement of spatial resolution, the additional access of several global and regional models to forecasters and the implementation of physical parameterisations that are well suited to polar phenomena has aided polar forecasters (Monaghan *et al.*, 2003). With such advancements in technology, the results from forecasts and simulations produced currently of the Antarctic are of much better quality than what was associated with modelling these areas a decade ago (Hines *et al.*, 1999). However, they are still not as accurate as those prepared for lower latitudes (Turner, 1996).

A prime objective for climate modellers is to understand the role of Antarctica in the global climate system. There are many globally significant processes that are driven by the unique climate and geography of the Antarctic region. Examples include the uptake of carbon dioxide by the Southern Ocean; the influence on the global ocean conveyor belt; the balance between storage and discharge of water in the continental ice sheet; and the modification of surface energy. Understanding processes such as these is vital for understanding and predicting climate and climate changes and their associated impacts. These impacts include issues such as greenhouse gas levels, sea level rise, atmospheric composition changes and the rate and variability of climate change.

To understand such processes that are driven by the Antarctic region, one first needs to look at the bigger picture, to understand how the unique surface of Antarctica interacts with the incoming shortwave and longwave radiation but also how this interaction affects the radiation and surface energy balances, not only on the regional scale, but on the global scale as well.

The radiation and surface energy balances

The radiation balance (or budget) is simply the balance between the incoming energy from the sun (also known as shortwave radiation, 0.15 - 3 μm) and outgoing energy from the Earth's surface (also known as longwave or terrestrial radiation, 3 - 100 μm). This can be further broken down by the following equation:

$$Q^* = (K\downarrow - K\uparrow) + (L\downarrow - L\uparrow)$$

Where Q^* = Net all wave radiation (limit to the available energy as a source or sink)

$K\downarrow$ = incident shortwave radiation

$K\uparrow$ = reflected shortwave radiation

$L\downarrow$ = incident longwave radiation

$L\uparrow$ = emitted longwave radiation

The radiation balance of snow and ice surfaces (as is present over 97% of the Antarctic surface) is complex. As opposed to most other surfaces, snow and ice allow a certain amount of shortwave radiation to penetrate the surface. This means that at any depth shortwave radiation can be transmitted, reflected or absorbed according to the following equation:

$$\psi + \alpha + \zeta = 1$$

Where ψ = transmissivity

α = reflectivity

ζ = apsorptivity (occurs within a volume rather than a planar surface)

The high albedo (or reflectivity) of snow and ice is arguably their most important and influential characteristic. The low energy status of snow and ice is a direct result of the high proportion of incident shortwave radiation that is rejected. The age of a snow pack can influence the amount of albedo measured. As a snow pack ages (becomes compacted and soiled) the albedo rapidly declines, but with fresh snowfall can increase again (Oke, 2000). For example, research conducted at King George Island, Antarctica, recorded that albedo was raised from 0.65 to 0.85 on the accumulation of fresh snow (Bintanja, 1995). During the summer, $K\downarrow$ is often more than

400 W m^{-2} on the Antarctic Plateau but due to the surface albedo being between 0.8-0.85, the net shortwave radiation is generally less than 80 W m^{-2} (King *et al.*, 1996).

For the long wave portion of the energy spectrum, snow and ice are almost full radiators. However, the magnitude of $L\uparrow$ is usually relatively small because T_0 (surface temperature) is low ($L\uparrow = \varepsilon_0 \sigma T_0^4$). With clear skies, net long wave radiation is almost always negative, similar to most other surfaces. The occurrence of frequent cloud cover exerts a major influence on the amount of $L\downarrow$ and $L\uparrow$. Frequent cloud cover in the King George Island example (Bintanja, 1995) caused temperature differences between the cloud and surface to be small; hence the net longwave radiation was comparatively small and less variable.

High albedo combined with a net long wave loss, results in a daily net radiation loss in Antarctica, even throughout early summer when day length is approximately 21 hours. For example, at midday net all wave radiation is less than 10% of the incoming solar radiation and the total daily net radiation is approximately -1 MJ m^{-2} d^{-1} (Oke, 2000).

Net all wave radiation is not only the end result of the radiation budget but also the basic input to the surface energy balance. Similarly to the radiation balance, the energy balance of snow and ice is complex, not only due to the penetration of short wave radiation but also by internal water movement and phase changes. Percolations of rainfall and meltwater production are the major forms of water movement within the snowpack or ice. Rainfall is very limited in Antarctica whereas meltwater production is more common, especially during the summer months. Phase changes (such as meltwater production) at any given location will involve energy losses or gains. When meltwater percolates through cracks in the ice it can freeze, when it does so it will release latent heat of fusion which his available to warm the surrounding ice.

Features such as those discussed above make it difficult to create an accurate surface energy balance for snow or ice. Oke (2000) suggests that a better approach is to construct a volume balance and to treat all fluxes as equivalent flows through the sides of the volume. If the horizontal energy transfers are ignored and volume is defined as extending from the surface to a depth where there is no significant vertical flux then the surface energy balance equation can be defined as:

$$Q^* = Q_H + Q_E + \Delta Q_S + \Delta Q_M$$

Where Q^* = net all wave radiation

Q_H = sensible heat

Q_E = latent heat

ΔQ_S = net heat storage

ΔQ_M = latent heat storage change due to melting or freezing

The net heat storage term is a representation of the convergence and divergence of sensible heat fluxes within the volume. This term includes internal energy gains or losses and heat conduction (concerns expressed earlier). ΔQ_M accounts for phase changes of water in the snow or ice volume.

It is important to note that the energy balance of a snow volume depends on whether it is a 'cold' (less than 0°C) or a 'wet' (more than 0°C, often isothermal) pack. For the 'cold' snowpack (most common in Antarctica) the amounts of ΔQ_M and Q_E are negligible. This is due to the fact that there is no liquid for evaporation, little vapour for condensation or sublimation, and the snowpack remains in the solid phase. Likewise heat conduction will be small due to low conductivity of snow and the lack of solar heating, therefore ΔQ_S is also negligible. As a result of the dominance of long wave exchanges, and the outgoing flux ($L\uparrow$) that is readily able to escape through the atmospheric window (no or little cloud due to lack of atmospheric water vapour and pollutants), the radiation balance is usually negative.

For global climate modelling it is essential that regional variations in the radiation balance and surface energy balance is known so that a better understanding of the phenomena that are common to certain regions can be gained. For example a better understanding of sensible heating of the land surface would be valuable to agriculture, hydrology and many other related fields. Regional variations in moisture availability (severely influenced by the surface energy balance) are a big influence on modelling of atmospheric phenomena. Surprisingly little is known about the spatial and temporal distribution of the surface energy balance over Antarctica (Reijmer and Oerlemans, 2000). Therefore in depth local and regional scale studies of the radiation and surface energy balances are needed for modelling purposes, especially over Antarcita.

MM5 - a state of the art climate model

The Fifth-Generation NCAR (National Center for Atmospheric Research)/PSU (Pennsylvania State University) Mesoscale Model (MM5) is a limited-area, hydrostatic/non-hydrostatic, terrain-following sigma-coordinate model designed to simulate (in this case study) or predict mesoscale

and regional-scale atmospheric circulation. The model is continuously being improved and has undergone many changes designed to broaden its usage.

Due to MM5 being a regional model, it requires initial conditions as well as lateral boundary conditions to run. To produce lateral boundary condition for the model to run, gridded data is required to cover the entire time period that the model is integrated (Pennsylvania State University / National Center for Atmospheric Research, 2005).

The MM5 model has been used in many regions and different climatic environments around the world. It has been used in Antarctica and the following example illustrates one of these. Monaghan and colleagues (2003) intended to inform the reader about several models commonly used in Antarctic weather prediction and to examine their performance in a notable forecasting event. In late April 2001, an unprecedented late-season flight to Amundsen-Scott South Pole Station was made to evacuate Dr. Ronald Shemenski, a medical doctor who was seriously ill (Powers *et al.*, 2003). This case study was used to analyse the performance of four numerical weather prediction models that aided meteorologists in forecasting weather throughout this mission: 1) the Antarctic Mesoscale Prediction System (AMPS) Polar MM5 (fifth-generation Pennsylvania State University-National Centre for Atmospheric Research Mesoscale Model), 2) the National Centres for Environmental Protection Aviation Model (AVN), the European Centre for Medium Range Weather Forecasts (ECMWF) global forecast model, and 4) the NCAR Global MM5. The results indicated that the following was the order of highest to lowest in overall predictive skill: 1) ECM, 2) AMPS, 3) AVN, and 4) GLO. At the surface, ECM exhibits the best performance, generally having the lowest values for bias and rmse, and the highest correlations. All four models demonstrate high skill in predicting surface pressure (correlations greater than 0.85), but moderate skill in predicting wind direction, wind speed, and temperature. AMPS has a systematic positive wind speed bias that is amplified during periods of light winds. All models capture the shifts in wind direction at South Pole, with AMPS and ECM showing the highest skill. This study shows that the MM5 model is a good predictor of surface conditions in Antarctica.

Aims

Few efforts have been made to produce detailed model verification statistics specifically for the Antarctic (Guo *et al.*, 2003)The aim of this study is to evaluate the simulations produced by the MM5 model by comparing with observations made at Scott Base during 25th to 31st October 2003 (a portion of the entire study period).

Methods

Micrometeorological observations were made during the period between 22nd October 2003 and 17th January 2004. The equipment was sited 316 m above sea level at position S78°00.907, E165°32.754. Measurements were recorded on a Campbell CR23X data logger and averaged at half hourly intervals. These observations included two levels of wind speed, temperature, and humidity. Incoming and outgoing shortwave and longwave radiation were measured directly using a Kipp & Zonen CNR1. The surface temperature was measured using an Everest infrared surface temperature sensor. Two Campbell 107 temperature probes were used to measure the subsurface temperatures; these were placed in the debris approximately 15 and 30 cm deep. It was noted that there was several bands of frozen ground at about 20-30 cm and that the ice surface was approximately 40 cm deep at this point (Penny Clendon, pers. comm.).

The simulations presented in this report were conducted with the MM5 (version 3.6.1) with the use of nonhydrostatic dynamics and polar projection. Three grids were used. Grid 1 (18 km spatial resolution) 81 x 81 x 27, Grid 2 nested (6 km spatial resolution) 121 x 121 x 27, and Grid 3 nested (2 km spatial resolution) 100 x 100 x 27. The sigma vertical co ordinate ranged from 0.998 (bottom) to 0.050 (top) (Mikail Titov, pers. comm.). The main physics parameters are shown in Table 1.

Table 1: Parameters used in MM5 modelling at Scott Base October 2003.

Parameters	**Description**
Physical parameterisation	Reisner mix phase scheme2 (grids 1-2)
	Dudhia simpe ice (grid 3)
Convection	MRF (ECMWF global model T-82 scheme)
PBL parameterisation	Blacadar scheme for high resolution grids
Radiation	RRTM (Rapid Radiative Transformation Method)
Soil model	Polar soil model with 7 layers from 5 cm to 150 cm
Radiation balance calculation frequency	10 minute intervals
Thermal roughness scheme in BL	Zilitinkevich scheme
Snow model	Switched on
Bucket soil moisture scheme	
Surface characteristics	Albedo = 0.45 (mean observed)
Roughness length over land	1 m
Roughness length over ocean	0.005 m
Surface thermal inertia	0.004

Results

Downward shortwave radiation

A cyclical pattern of downward shortwave radiation (K↓) is evident (Figure 1). The results when plotted form a curve that usually climbs and recedes at a constant rate, except for spikes (both above and below what is expected) that usually occur in the afternoon, an exception being the 29th and 30th of October (observations were variable and did not follow the smooth curves as the other days did). Observed K↓ tends to peak at 1200 h with values being between 470 W m^{-2} and 540 W m^{-2}. The lowest recordings were generally made between 2300 h and 0400 h, with observations being less than 50 W m^{-2}.

The modelled simulations followed a very similar cyclical pattern for K↓. On day 2 and 3 the values for K↓ seem to be lagging between half an hour and an hour behind the observations (this only occurs up until approximately 1300 h). The modelled results for days 4 and 6 also seem to be lagging behind the observations, in this instance approximately 1.5 h behind. Days 1 to 3 have modelled plots that are very smooth that are essentially mirror images of each other. The remaining modelled K↓ plots follow the similar patter but have much more variation between 0900 h and 1500 h.

Table 2 is an indication of the maximum, minimum, mean and correlation coefficient for K↓ for observations and modelled results.

Table 2: Statistical analysis of observed and modelled results for downward shortwave radiation.

	observed	modelled
Minimum	5.3	0.0
Maximum	535.4	478.0
Mean	216.2	199.9
Correlation coefficient		0.97

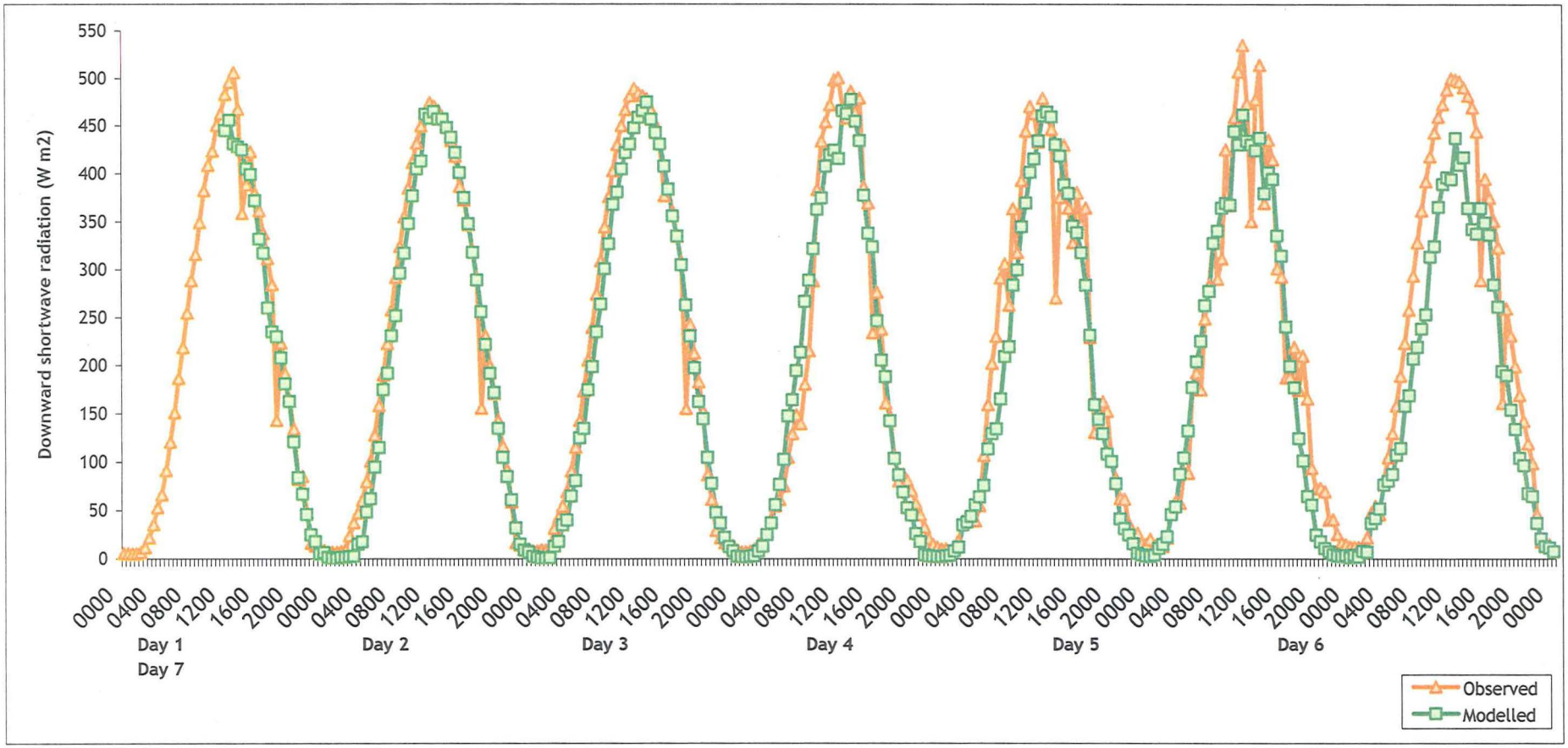

Figure 1: Graph of observed and modelled downward shortwave radiation

Upward shortwave radiation

Upward shortwave radiation ($K\uparrow$) also tends to follow a cyclic pattern (Figure 2). Note that it is convention to graph upward radiation (both K and L) as negative, the values are not negative it only indicates that it is outgoing as opposed to incoming. During days 1 to 3, $K\uparrow$ tended to range between 3 W m^{-2} to 180 W m^{-2}, with the individual data points joining up to form smooth curves. On days 4 to 6, $K\uparrow$ was much more variable and the largest recording was made on the 28th, being 242.6 W m^{-2}. From midday on the 30th onward, observed $K\uparrow$ tended to resemble a smooth curve when results plotted.

Modelled results for $K\uparrow$ also display the typical cyclic pattern, whereby increasing throughout the morning, peaking then declining at approximately the same rate. For the first three days the maximum amount of $K\uparrow$ was generally equal, roughly 190 W m^{-2}. During days 4 to 7 the maximum amount of $K\uparrow$ greatly increased to approximately 240 W m^{-2}. During the daily minimum, at no stage did $K\uparrow$ fall below 0.5 W m^{-2}.

Table 3 is an indication of the maximum, minimum, mean and correlation coefficient for $K\uparrow$ for observations and modelled results.

Table 3: Statistical analysis of observed and modelled results for upward shortwave radiation.

	observed	modelled
Maximum	242.6	251.0
Minimum	2.8	0.5
Mean	87.9	103.2
Correlation coefficient		0.95

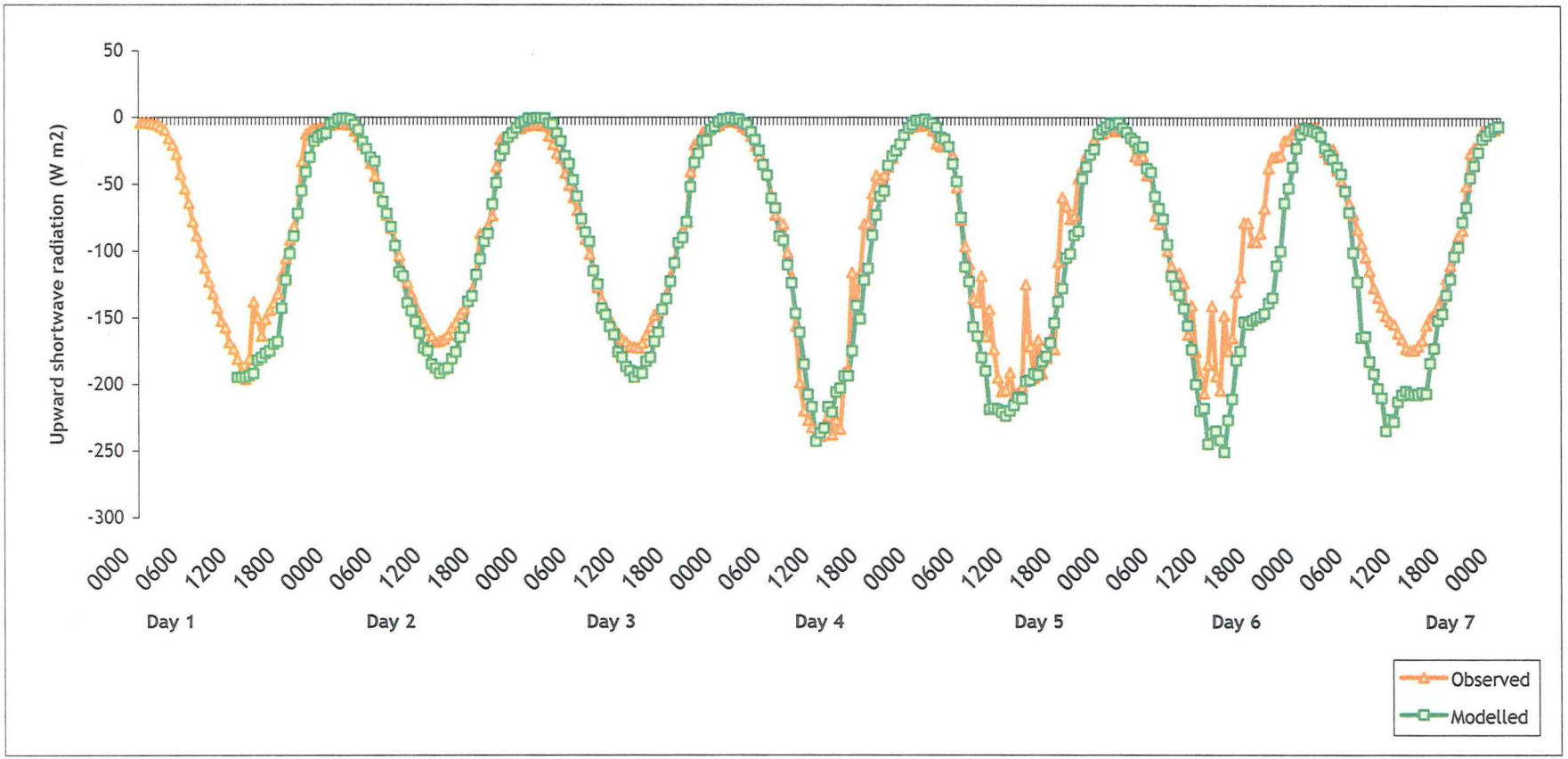

Figure 2: Graph of observed and modelled upward shortwave radiation

Downward longwave radiation

Observed downward longwave radiation (L↓) is quite variable and no pattern appears to exist (Figure 3). Days 1 to 3 display relatively similar values for L↓, generally being 135 W m^{-2} to 170 W m^{-2}. Short term spikes (from one hour to the next) in the daily plots are not evident, in comparison days 4 to 6 indicate that values of L↓ are far greater in magnitude and are of a much more variable nature, even on an hourly basis. For example, on day 3 at 2300 h L↓ was 140 W m^{-2}, one hour later L↓ was 220 W m^{-2}.

During the first three days of simulations, modelled results for L↓ seem to vary very little, only in the order of 25 W m^{-2}. Variation on an hourly basis is hard to distinguish, results tend to gradually increase, decrease or remain status quo. From day 4 onwards, values for L↓ are much more extreme, hence there are larger variations on a day to day basis. It appears that the minimum values obtained for L↓ are relatively similar (approximately 150 W m^{-2}), but that the maximums are much more variable (ranging from 170 W m^{-2} on day 2 to 228 W m^{-2} on day 6).

Table 4 is an indication of the maximum, minimum, mean and correlation coefficient for L↓ for observations and modelled results.

Table 4: Statistical analysis of observed and modelled results for downward longwave radiation.

	observed	modelled
Minimum	128.5	146.0
Maximum	236.3	228.0
Mean	169.3	172.0
Correlation coefficient		0.66

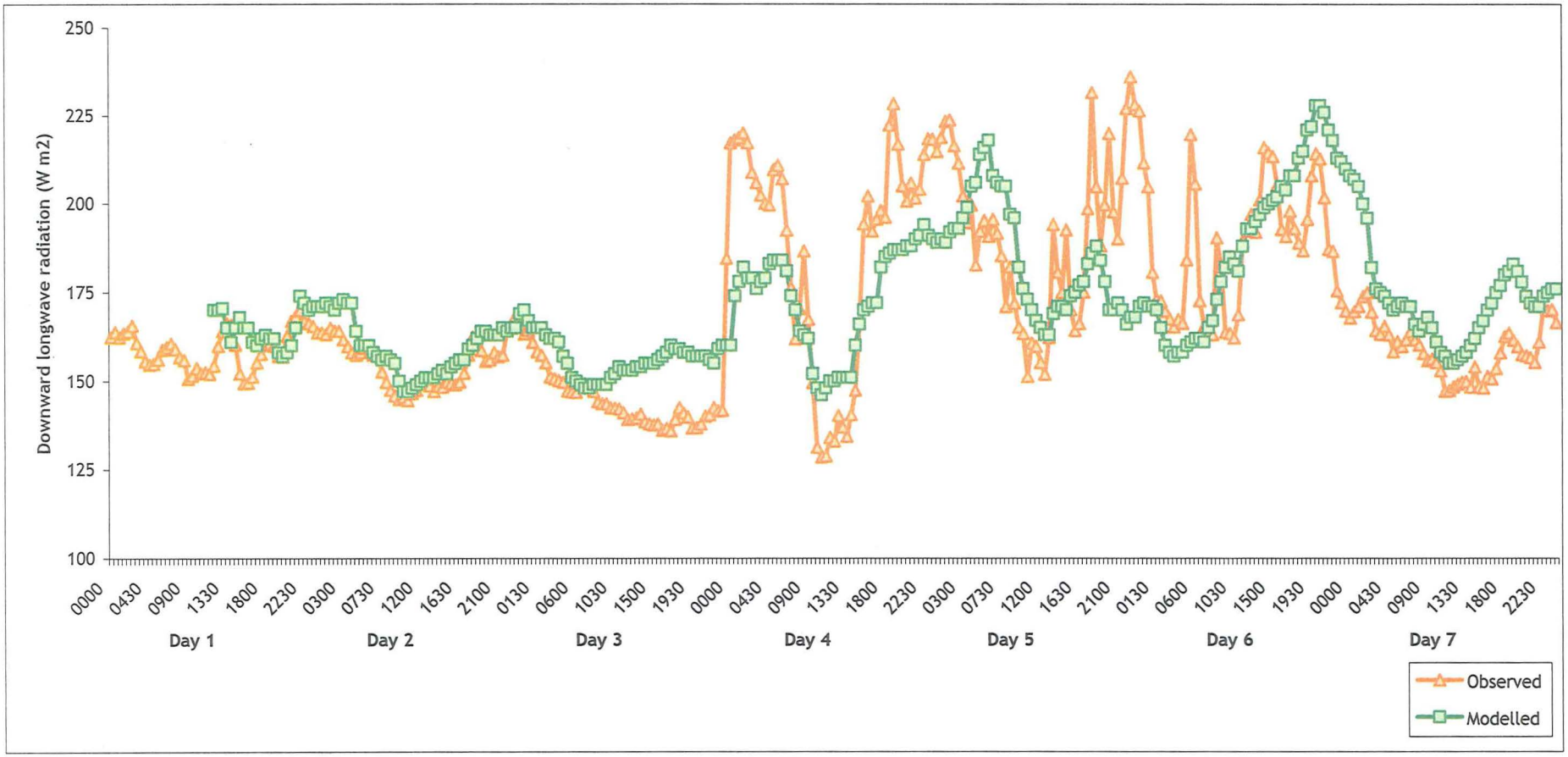

Figure 3: Graph of observed and modelled downward longwave radiation

Upward longwave radiation

Upward longwave radiation ($L\uparrow$) follows a similar pattern each day (Figure 4). 2000 h seems to be the approximate time when $L\uparrow$ is at its maximum, usually around 275 W m^{-2}. This is similar to a study conducted Bintanja and Van Den Broeke (1995) who found that $L\uparrow$ was greatest around 1800 h. After 2000 h $L\uparrow$ rapidly decreases to a daily minimum at approximately 0400 h. The observed value for $L\uparrow$ tends to be around 220 W m^{-2}. Between 0400 h and 2000 h, $L\uparrow$ gradually increases. Days 1 and 2 follow a very similar pattern with almost identical values throughout the day. Days 3 and 4 also follow the similar daily cycle as previous days except the maximum and minimum observations are less extreme as the previous two days. Days 5 and 6 are also less extreme in amounts observed and do not have the sharp decrease of $L\uparrow$ from 2000 h to 0400 h that was observed previously. The maximum recorded $L\uparrow$ occurs earlier as well, at approximately 1530 h on both days. Day 7 follows a similar pattern as the first two days but has more extreme values.

Modelled results for $L\uparrow$ indicate that there is a daily pattern, with $L\uparrow$ at its maximum between 1430 h and 1630 h, with the trough at approximately 0300h, and then increasing at a similar rate. An exception to this is the rate of change for $L\uparrow$ between day 4 and 5. The amount of $L\uparrow$ increases at a constant rate (slower than previous days) throughout the rest of day 4 (after 1430 h) and into day 5. The minimum amount of $L\uparrow$ does not occur until 0700 h, approximately 4 hours later than the other days. A rapid increase in $L\uparrow$ then occurs, peaking at the usual time. Day 7 does not exhibit the usual modelled trend, it seems to 'peak' at a similar value many times throughout the day.

Table 5 is an indication of the maximum, minimum, mean and correlation coefficient for $L\uparrow$ for observations and modelled results.

Table 5: Statistical analysis of observed and modelled results for upward longwave radiation.

	observed	modelled
Minimum	286.3	236.0
Maximum	219.7	179.0
Mean	246.7	208.9
Correlation coefficient		0.29

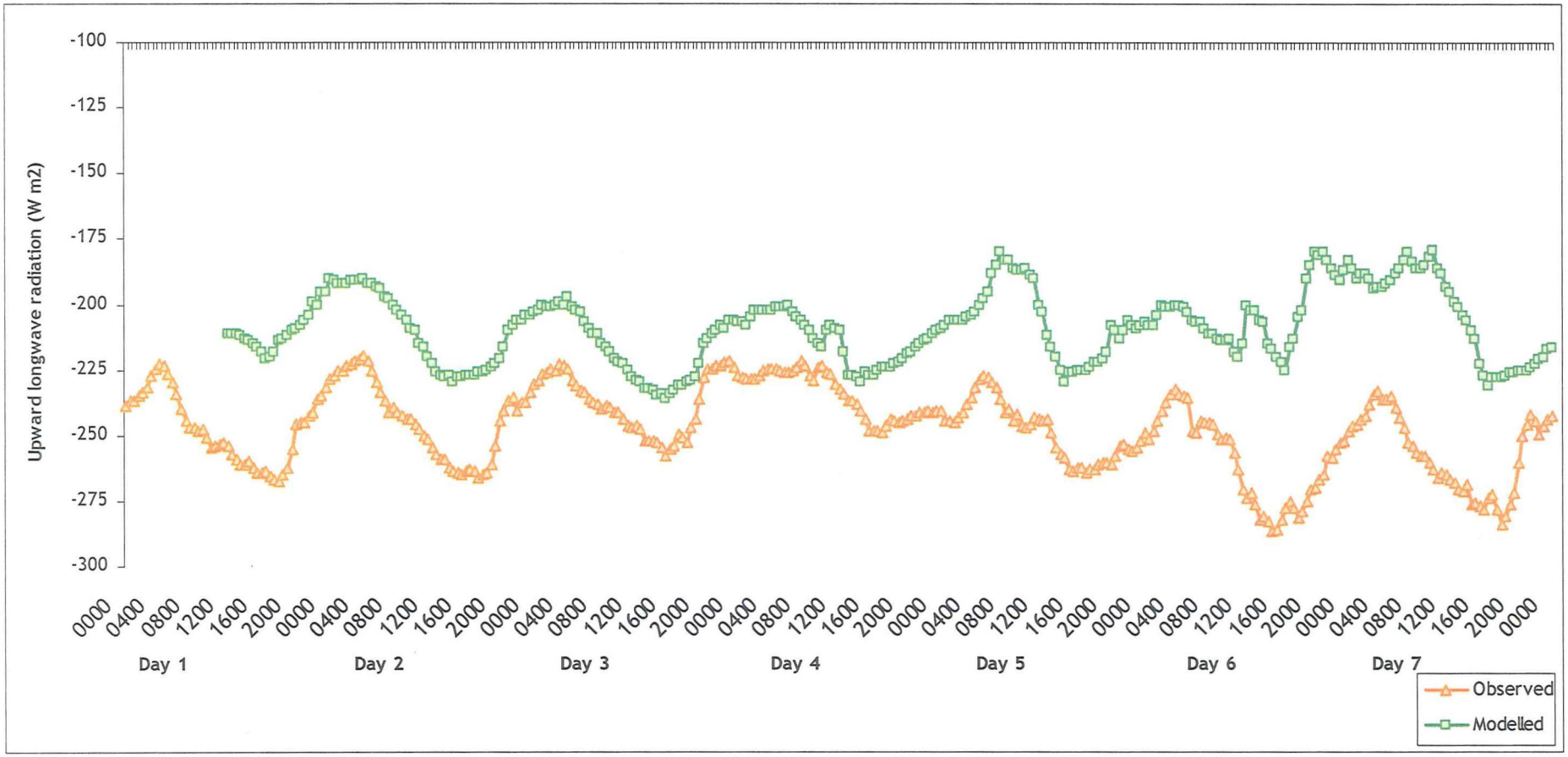

Figure 4: Graph of observed and modelled upward longwave radiation

Net radiation (Q)*

Observed net radiation tends to follow a typical trend of increasing Q* throughout the day, peaking at approximately 1200 h, then decreasing amounts of Q* at approximately the same rate. The difference between minimum and maximum Q* throughout the day is quite substantial, usually in the range of 270 W m^{-2}. Minimum observations of Q* usually occur between 2200 h and 2300 h, usually in the range of -60 W m^{-2} to -70 W m^{-2}. The peak in Q* as mentioned earlier usually exists at about 1200 h and is usually in excess of 200 W m^{-2}. All of the days have spikes in the net radiation plots, quite often just in the afternoon hours. It is also common for the net radiation to enter negative values, sometimes only for an hour then return back to its previous positive position. Days 1 to 3 are all very similar in plots and magnitude, all plots have a smooth rapid increase, peak then decrease at a similar rate with spikes in observed net radiation. Days 4 to 6 are much more variable from hour to hour and over the three days, the peak net radiation gradually increases. Day 7 is much the same as days 1 to 3.

The modelled results follow a similar net radiation plot with values increasing throughout the day, peaking, then following a similar decline throughout the remaining hours. Peak modelled results for Q* are usually in excess of 200 W m^{-2}, minimum values are usually around -40 W m^{-2}. Days 1 to 3 follow the typical plot with little variation from hour to hour, only a few spikes are evident. Days 4 to 6 still follow the typical plot but are much more variable from hour to hour. The peak Q* for day 6 lasts longer than the usual one recorded value (with steep increases and decreases on either side). On day 7 Q* is relatively stable until 0900 h when values rapidly increase. After the peak the Q* plot is much more similar to the other modelled days.

Table 6 is an indication of the maximum, minimum, mean and correlation coefficient for net radiation.

Table 6: Statistical analysis of observed and modelled results for net radiation.

	observed	modelled
Minimum	-74.9	-62.0
Maximum	247.4	220.0
Mean	51.4	59.7
Correlation coefficient		0.89

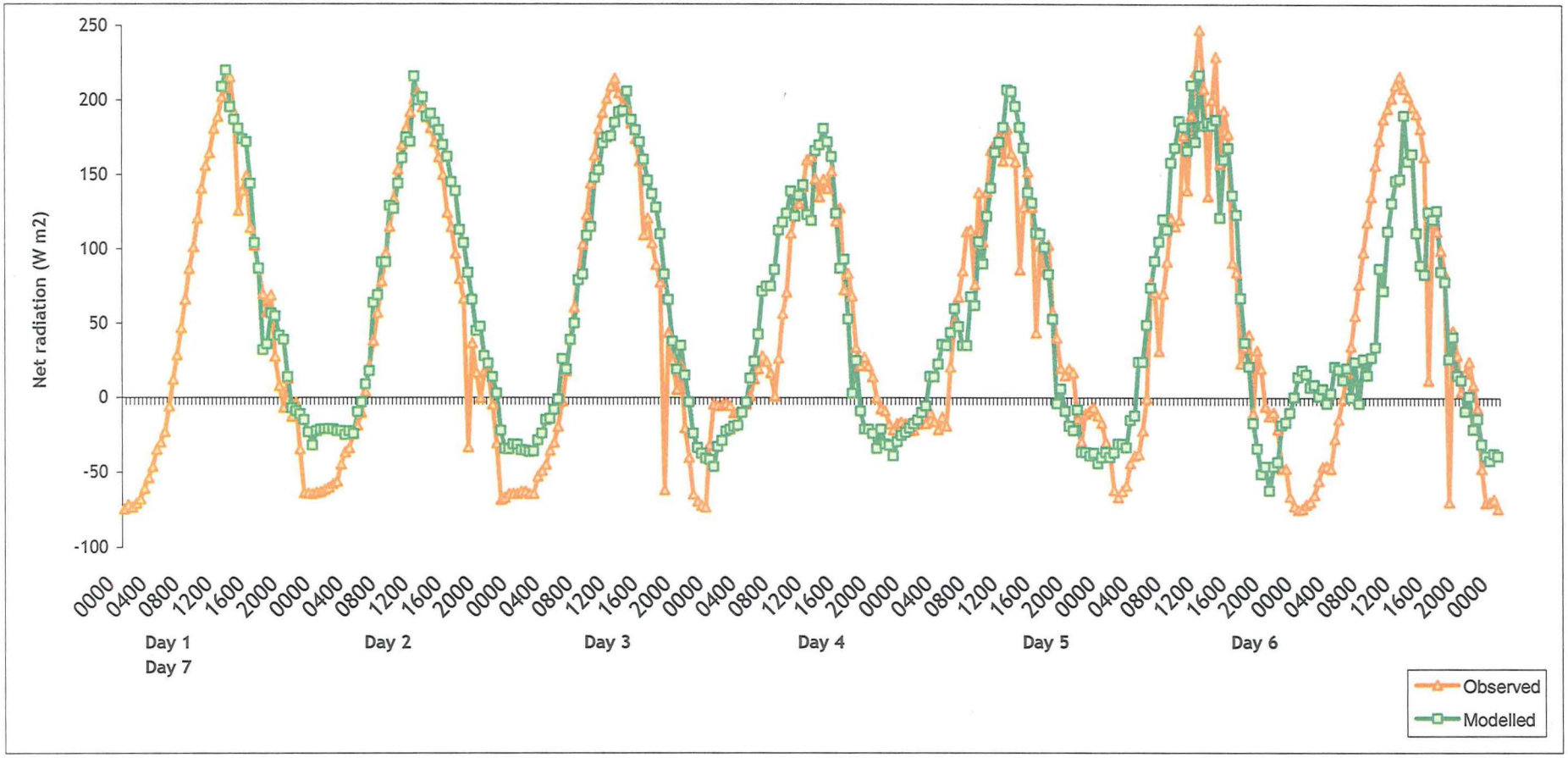

Figure 5: Graph of observed and modelled net radiation.

Sensible Heat Flux

There does not seem to be any apparent daily pattern of the sensible heat flux (Q_H) (Figure 6). Observed values tend to vary between 0 W m^{-2} and 10 W m^{-2}, with the occasional negative spike. The negative spikes would most often only last for an hour or so, with the exception being on days 1 and 2 when a negative Q_H was measured constantly for approximately 5 hours. On days 4 and 5 very small amounts Q_H were measured, with little variation occurring. On days 1, 6 and 7 observations of Q_H were quite variable, with some negative observations being recorded.

The degree to which modelled Q_H varies between daily extreme values is quite considerable. For example on day 4 Q_H varies from a minimum of -22 W m^{-2} at 0300 h to a maximum of 54 W m^{-2} at 1600 h. More often than not modelled Q_H follows a typical daily pattern. This entails a minimum Q_H modelled between 0200 h and 0300 h, a peak at between 1500 h and 1600 h, then at a similar rate, a decline to the minimum. Days 1, 2, 4 and 7 all follow a similar pattern of increasing and decreasing amounts of Q_H. Day 3 is similar but its magnitude is much less, and also the difference between extremes throughout the day is less. Day 4 undergoes a rapid increase in Q_H between 0300 h and 0530 h. Near the end of day 5, an unusual spike in modelled Q_H occurs between 2200 h and 0200 h when Q_H should be continuously decreasing. Day 6 also incurs a slight increase in Q_H, in this instance from 2200 h to 0000 h.

Table 7 is an indication of the maximum, minimum, mean and correlation coefficient for Q_H for observations and modelled results.

Table 7: Statistical analysis of observed and modelled results for sensible heat flux.

	observed	modelled
Minimum	-25.7	-25.0
Maximum	10.4	54.0
Mean	1.6	6.4
Correlation coefficient		0.24

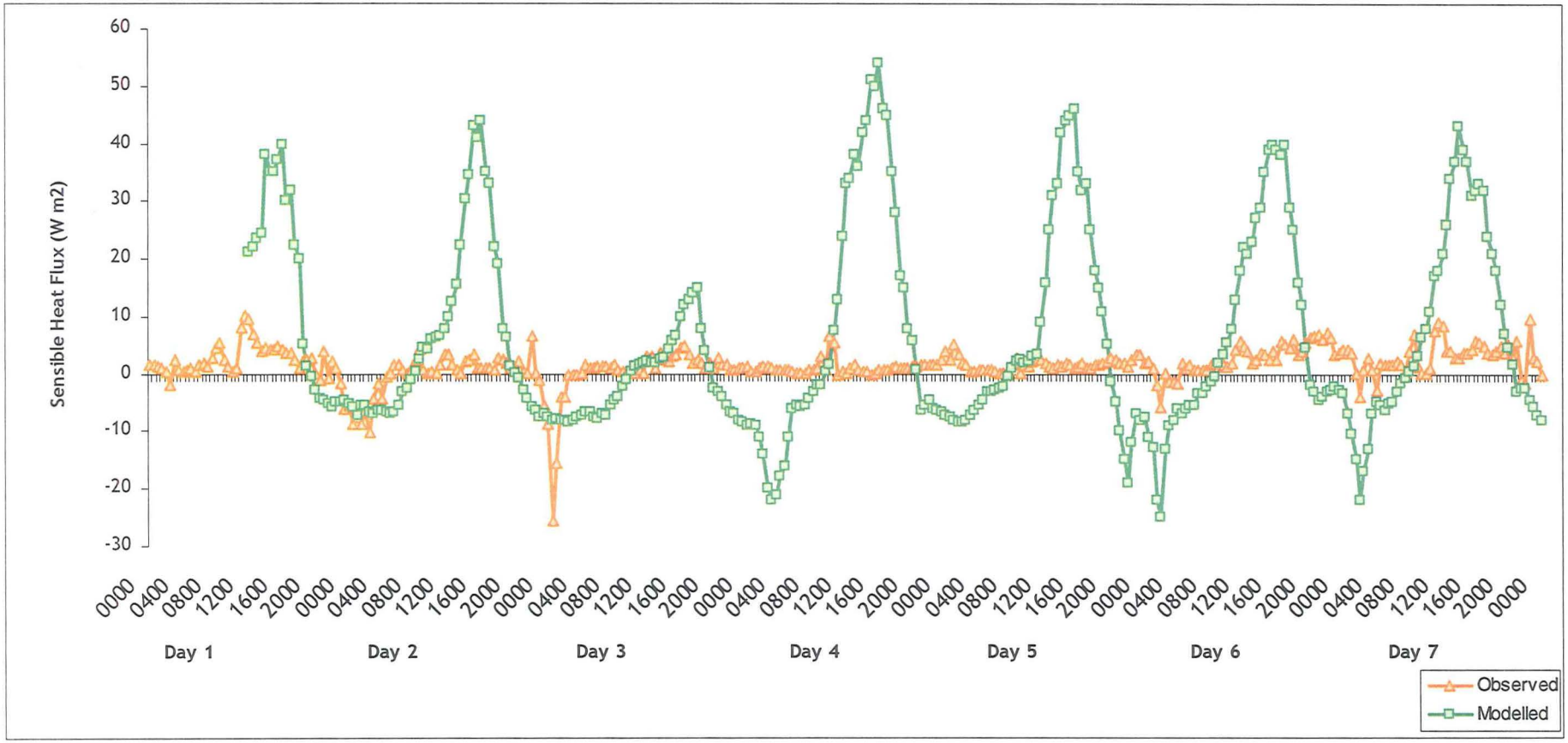

Figure 6: Graph of observed and modelled sensible heat flux

Latent heat flux

The observed latent heat flux (Q_E) changes very little throughout the entire study period (Figure 7). The values are constantly between 0 W m^{-2} and -0.1 W m^{-2}. Negative observations of Q_E tend to occur during the late hours of the day (post 2200 h) and early morning (prior to 0300 h). Other than this, no apparent diurnal cycling occurs. Negative spikes usually last for approximately 1-2 hours, the exception being day 2/day 3 where negative observations lasted from 2200 h to 0100 h. Bintanja and Van Den Broke (1995) also measured a negative latent heat flux throughout the day in Dronning Maud Land, they conclude it is a result of heat loss through sublimation.

As can be seen in Figure 7, modelled Q_E does not vary at all over the entire study period, except for a big spike on day 2. All other values for Q_E are modelled to be 0 W m^{-2}. At 0600 h there is a modelled Q_E of 0.1 W m^{-2}, results drop back down to 0 W m^{-2} for the next 3.5 hours. Between 0930 h and 1000 h Q_E rapidly increases to 0.7 W m^{-2} where relatively high results are sustained until a peak value of Q_E is reached of 1 W m^{-2} at 1200 h. By 1430 h Q_E is simulated to be back at 0 W m^{-2} where it remains for the rest of the study period.

Table 8 is an indication of the maximum, minimum, mean and correlation coefficient for Q_E for observations and modelled results.

Table 8: Statistical analysis of observed and modelled results for the latent heat flux.

	observed	modelled
Minimum	-0.2	0.0
Maximum	0.0	1.0
Mean	0.0	0.0
Correlation coefficient		0.1

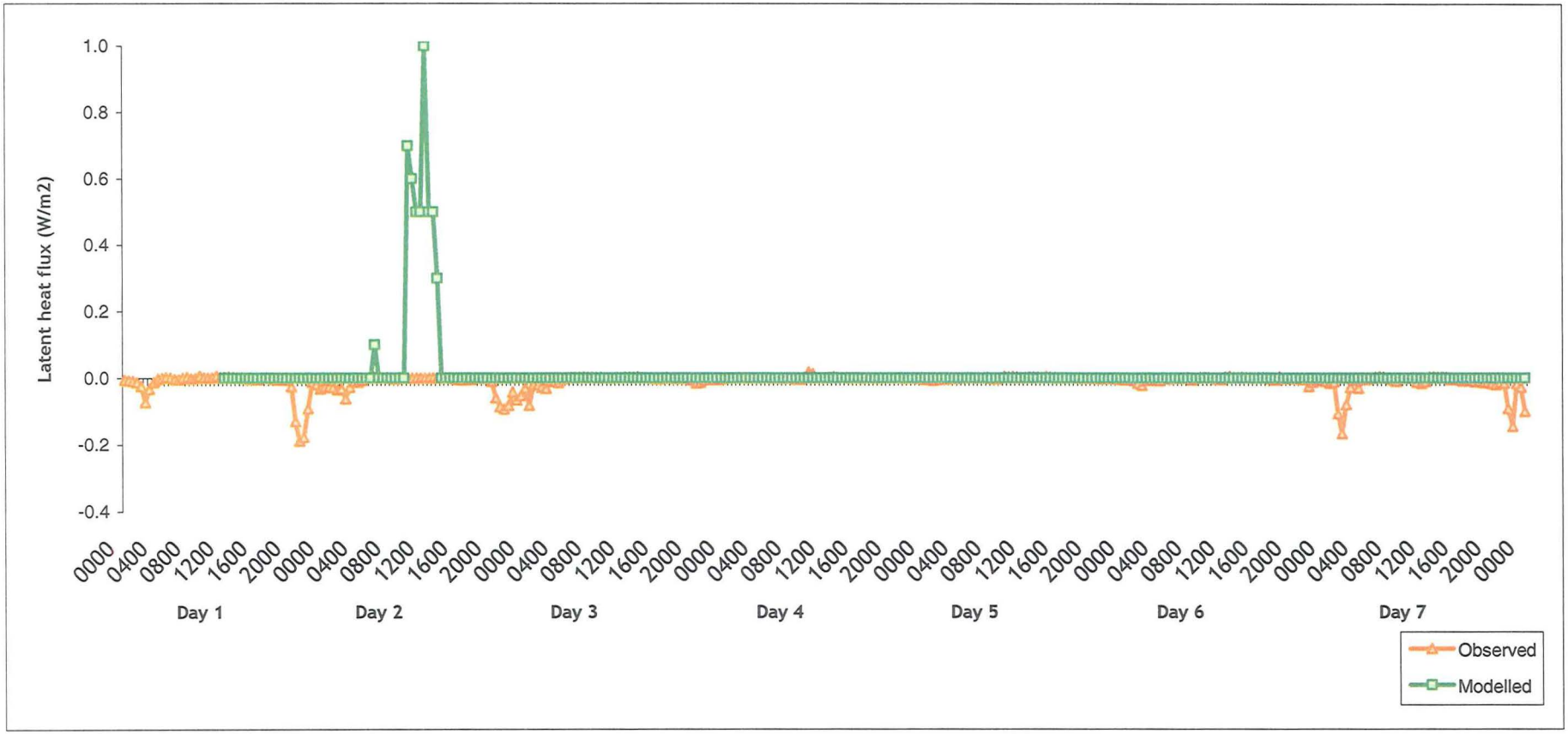

Figure 7: Graph of observed and modelled latent heat flux

Wind direction

The observed wind direction looks quite variable when analysing Figure 8, however there are times when the wind direction is relatively constant (days 2 and 4 in afternoon and day 3 early morning and late night). Wind direction seems to be most common from the northeast, northwest and southeast. On day 1 wind direction was extremely variable from hour to hour. Day 2 saw morning wind directions from the east, with a shift in direction to a northwesterly. Wind direction on day 3 saw southeasterlys up until 1500 h, followed by a northeasterly until 1930 h. The wind direction then shifted back to an easterly. Throughout the early morning until 0900 h on day 4 observed winds were coming from the southeast. For the rest of the day, wind direction shifted to a northwesterly. Within two and a half hours in the early hours of day 5, wind direction changed from a northwesterly to a northeasterly.

Day 2 saw a shift in wind direction from the southeast to the afternoon which had a westerly component. Wind direction on day 3 varied little, generally coming from the southeast. The early hours of day 4 saw wind directions continuing from the southeast, for the remainder of the day winds were recorded coming from the west to northwest. From 0000 h until 0630 h on day 5, wind direction was modelled to be shifting from a southerly to an easterly. From this point until 1400 h, wind direction varied between a northeasterly and an easterly. The night was modelled to have shifts in direction from the southwest then a northwesterly. Day 6 had wind directions modelled coming from the southwest in the early hours, then a southeasterly for the remainder of the day. When wind directions for day 7 were modelled the result was wind directions generally coming from two directions, the west and southeast.

Table 9 is an indication of the maximum, minimum, mean and correlation coefficient for wind direction for observations and modelled results.

Table 9: Statistical analysis of observed and modelled results for wind direction.

	observed	modelled
Minimum	35.8	47.0
Maximum	327.8	348.0
Mean	160.8	169.7
Correlation coefficient		0.80

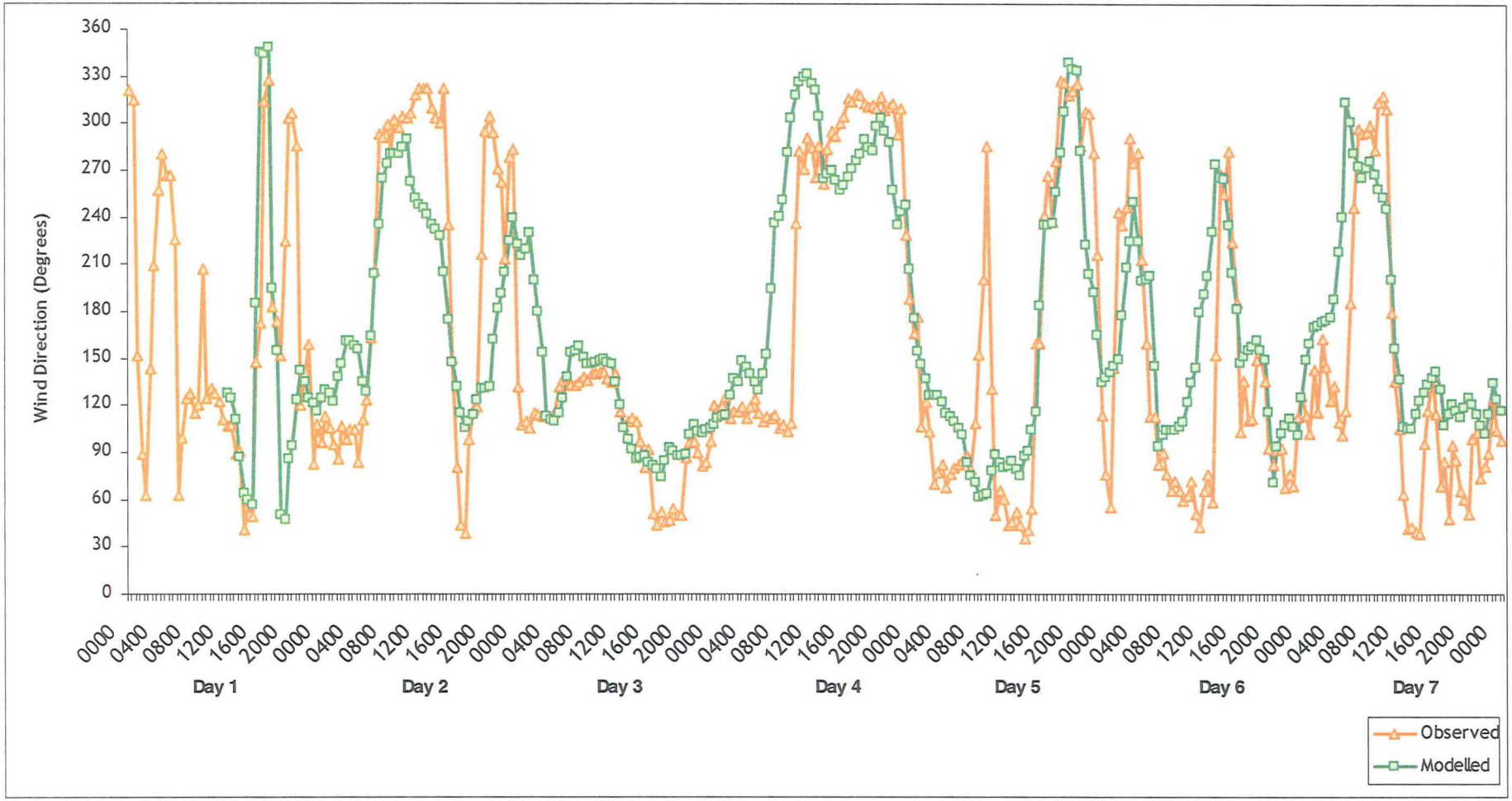

Figure 8: Graph showing observed and modelled wind direction

Surface temperature (°C)

Surface temperature varied on a cyclic pattern during the day (Figure 9). The maximum daily ground temperature seemed to occur between 1430 h and 1600 h, varying from -7°C to 5.5°C. The daily minimum occurred around 0300 h, with the observation always being approximately -20°C. Days 4 and 5 had much lower maximum temperatures than the other days, being approximately 6C less than the others. Days 1, 2, 6 and 7 all recorded positive maximum temperatures. Most days had an interesting kink in the smooth curves created by half hourly observations. Between 0000 h and 0400 h, temperatures would gradually decrease to their daily minimum. From 0400 h to 0830 h, temperatures would then start to increase at the same gradual rate. Suddenly the recorded surface temperature would drop for approximately two hours, would gradually increase for a further two hours, then rapidly increase to the daily maximum at approximately 1500 h. Temperatures would not stay at this peak value for long, then rapidly recede back to their minimum. Days 4, 5 and 6 were more variable throughout the day but this general pattern could be observed throughout the noise.

When all modelled data points were joined up, the daily cycle usually followed a smooth increase then decrease in ground temperature as the day progressed. Days 1, 2 and 3 followed very similar daily progressions with similar temperatures being simulated. Day 4 had the least variable modelled temperature extremes. Days 5 to 7 seemed to incur a gradual increase in modelled temperatures, the minimum temperatures kept approximately the same, but the maximum temperatures increased by approximately 5°C each day.

Table 10 is an indication of the maximum, minimum, mean and correlation coefficient for surface temperature for observations and modelled results.

Table 10: Statistical analysis of observed and modelled results for surface temperature.

	observed	modelled
Minimum	-21.2	-19.4
Maximum	5.5	0.2
Mean	-12.5	-11.1
Correlation coefficient		0.89

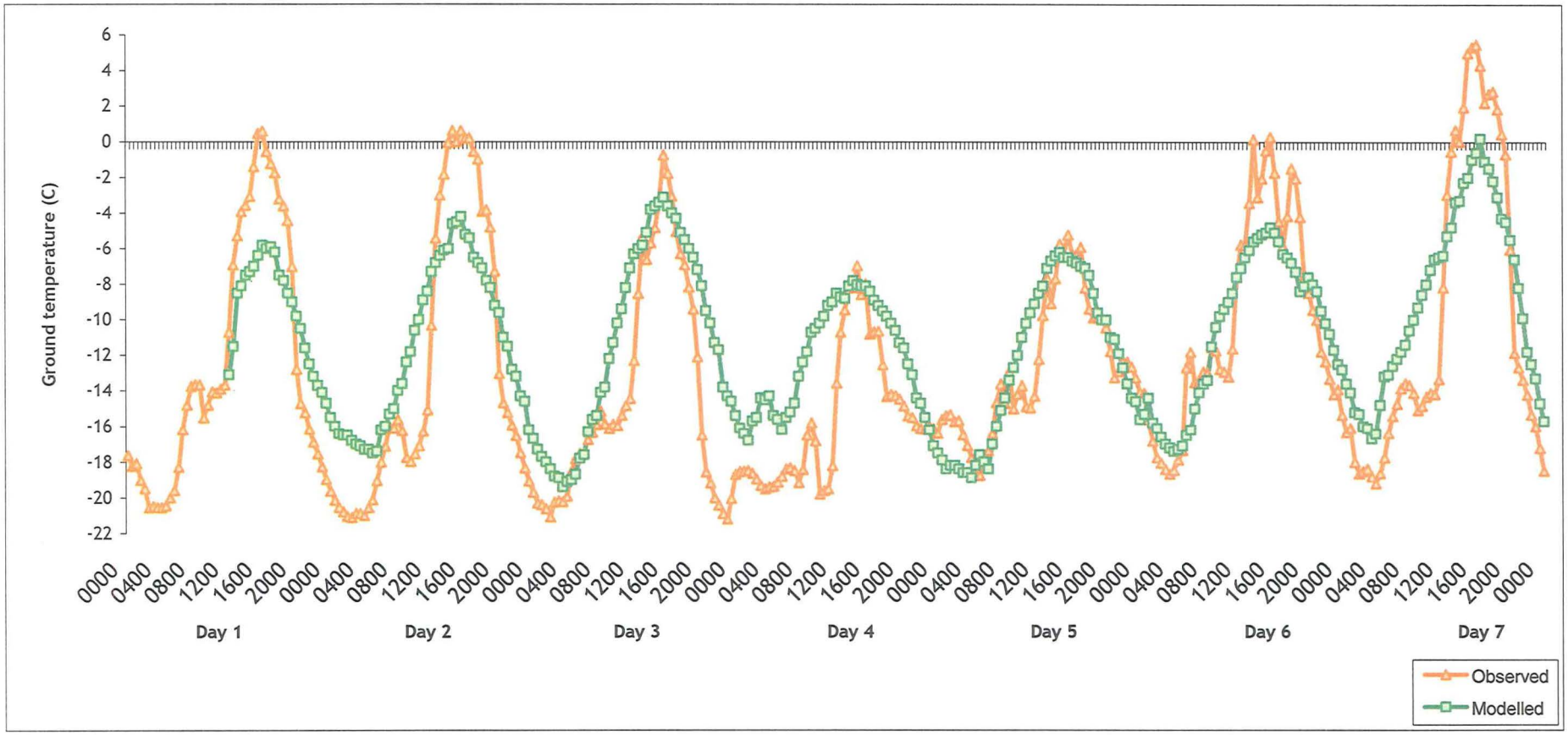

Figure 9: Graph of observed and modelled ground temperature

Air temperature at 2 m

Observed air temperature at 2 m generally increases throughout the morning to peak between 1500 h and 1630 h (Figure 10). The recorded temperature then decreases throughout the rest of the day. Temperatures are usually at their minimum between 0200 h and 0400 h. Air temperatures are much more variable from hour to hour compared with the recorded ground temperature. Temperature trends for days 1 and 2 follow a gradual increase then decrease throughout the day. On day 3 air temperatures gradually increased to their maximum, then declined at a more rapid rate than previous days. The difference in minimum temperature between day 2 and 3 was approximately 3°C. On day 4 temperatures rapidly increased between 0500 h and 0930 h, but throughout the rest of the day, temperatures remained relatively constant. Day 5 followed a similar temperature plot as day 4 but temperatures rose to a greater extent. Day 6 followed the typical temperature increase and decrease, as did days 1 and 2. The temperature extremes were much less variable and minimum temperatures between days 5 and 6 was approximately 7°C. Day 7 also did not have the variation in extremes of temperature and also did not have the typical increase, peak then decline in temperature.

The modelled air temperature generally followed the characteristic increase, peak then decline in temperatures. Minimum modelled temperatures ranged from -19°C to -12°C. Temperature plots for days 1, 2 and 3 are very similar in magnitude, varying by approximately 2°C in maximum temperature. Days 5, 6 and 7 follow similar plots and each day represents approximately 3C temperature increase for maximum temperature modelled. Minimum temperatures increase by as much as 6°C (between minimum on day and minimum on day 7).

Table 11 is an indication of the maximum, minimum, mean and correlation coefficient for air temperature at 2 m for observations and modelled results.

Table 11: Statistical analysis of observed and modelled results for air temperature at 2 m.

	observed	modelled
Minimum	-22.5	-19.4
Maximum	-5.9	-4.5
Mean	-14.5	-11.8
Correlation coefficient		0.81

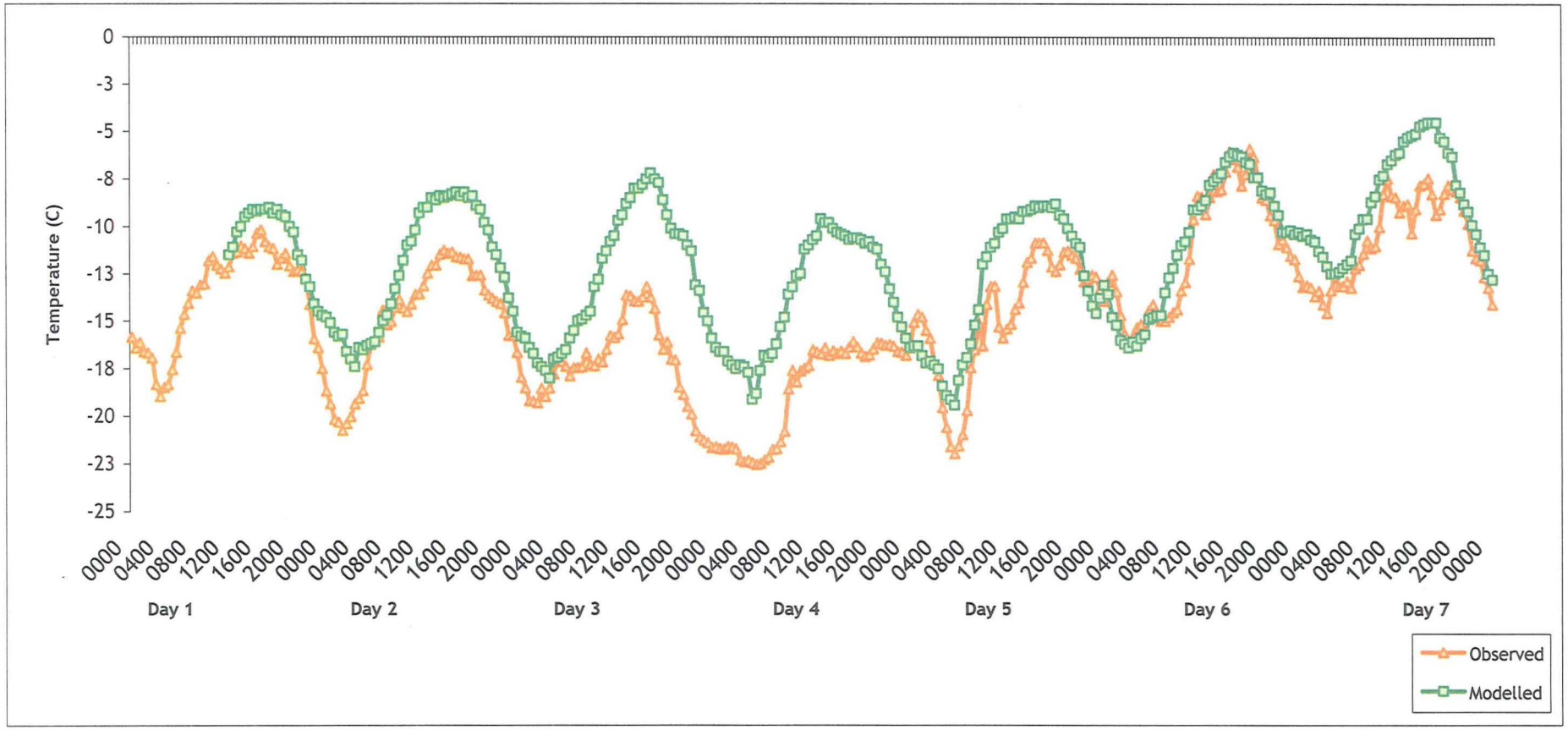

Figure 10: Graph of observed and modelled air temperature at 2 m.

Discussion

Downward shortwave radiation

The modelled results for K↓ mimic extremely well what the observations show. Days 2, 3, 5 and 7 indicate that the upward limb of the modelled K↓ is lagging behind observations, in the first three cases approximately 2 hours, the latter example up to four hours. The downward limb on most days seems to be in better agreement with the observations (the exception being days 6 and 7). On the first four days when observation curves are relatively smooth, the modelled results fail to register spikes in the data set. On all of the days studied, the model does not simulate the same magnitude of the peak; it does a descent job, but underestimates by as much as 70 W m^{-2} on day 6. Table 2 indicates some statistics conducted on the modelled results and observations. As shown by the high correlation coefficient of 0.97, the model does a very good job of simulating the observations of K↓. The table also shows how the model slightly overestimates the minimum K↓ and substantially underestimates the maximum; therefore the modelled mean is slightly lower than expected.

The model's tendency to underestimate the peak K↓ could lead to surface temperatures which are modelled to be too cold and therefore an underestimation of L↑ (as it severely depends on surface temperature). This occurs at the Carrefour site (Massachusetts Institute of Technology , 2004). In the Scott Base example there is an underestimation of peak K↓ and an underestimation of L↑, however the modelled surface temperatures do not indicate that the temperature is colder than what was expected from the observations. The underestimation of L↑ and K↓ must be a function of the parameters used in the model.

Upward shortwave radiation

The modelled results for K↑ also follow very similar curve plots and magnitudes with what observations show. During days 1 to 3, the modelled simulations follow very similar plots to observations. The model however does not register the big spike identified from observations on day 1. From day 4 onward the model simulates the general daily pattern but does not simulate the individual fluctuations well. On days 6 and 7 the model simulates a period of time (approximately 1600 h to 2000 h) where K↑ changes very little; this is not reflected in the

Upward longwave radiation

The model does a great job at simulating the general daily cycle of L↑ that was observed, but underestimates the amount of L↑ that is leaving the surface. During the first four days, the model under estimates the amount of L↑ by approximately 30 W m^{-2}. Days 5 to 7 indicate that the model is having a more difficult job at accurately simulating the daily magnitudes of L↑, at its maximum the model underestimates by approximately 70 W m^{-2}. The model also tends to simulate the maximum daily L↑ approximately 2-3 hours earlier than what is observed. As a result of the model always underestimating the magnitude of L↑ the correlation coefficient between the observations and modelled results is only 0.29.

The Joint Program on the Science and Policy of Global Change from the Massachusetts Institute of Technology (Massachusetts Institute of Technology, 2004) did a comparison study between observations and model estimates for radiation and surface energy balance for ETH Camp (Greenland) and the South Pole (Antarctica). They state that because the upward longwave radiation flux depends only on the surface snow temperature (blackbody emission, the emissivity of snow and ice is very close to one in the infrared part of the spectrum), which is in turn determined by the net surface energy balance, the upwelling longwave radiative flux provides a very good indicator of the overall quality of that balance. If this statement is true as expected, then the modelling parameters used during the case study at Scott Base need to be adjusted so that the upward longwave radiation flux is in greater agreement with observations. This will provide more accurate simulations and therefore will increase the accuracy of the surface energy balance calculated from these modelled results.

Net radiation

The model does quite a good job at simulating Q* over the study period. The general daily cycle of Q* is modelled well, with the receding limb on days 2, 3 and 4 lagging behind, while the rising limb on days 4 and 5 is ahead of observations, and on days 6 and 7 is behind observations. On every day except day 4, the model underestimates the minimum Q* that is observed. For the maximum daily Q*, the model usually does a good job at simulating a similar magnitude. The modelled results for day 7 would worst example over the study period, with the model simulating spikes when they were not observed (especially in the morning), overestimating the minimum Q* and underestimating the peak Q*. The correlation coefficient for Q* is 0.89, this means that the model did a good job at simulating the observed results.

Sensible heat flux

The model does not do a good job at modelling the changes in Q_H over the study period. The model simulates a large peak in Q_H each day at approximately 1600 h, this does not agree with the observations made, where no pattern is apparent. For example on day 4 the modelled simulated 54 W m^{-2} compared to the observed 0.1 W m^{-2}. The model simulates negative Q_H for much longer than what is observed (approximately 12 hours modelled compared to 2-3 hours observed), and to a more extreme value (for example on day 4, -22 W m^{-2} was the modelled minimum compared to 0.1 W m^{-2} that was observed) sometimes simulating negative Q_H when it is not observed (for example, day 5). The lack of plot agreement is reflected in the statistical analysis performed (Table 7). The correlation coefficient is a insignificant 0.24. The model does a good job at simulating the minimum Q_H but an awful job at modelling the maximum. For this reason, the modelled mean is much higher than the observed.

A study by Lewis and colleagues (1998) is in agreement with the low observed sensible heat flux. The average Q_H measured between 22nd November and 10th January (1995-1996) at the Canada Glaicer, Taylor Valley, Antarctica was 3.01 W m^{-2}. This is similar to the Scott Base case study of 1.6 W m^{-2}.

As can be deduced from the above discussion of the sensible heat flux, the Scott Base case study indicates that Q_H was found to be directed towards the surface throughout almost the entire period. This observation is in agreement with a study conducted by Bintanja (1995) on the Ecology Glacier, King George Island, Antarctica. He concluded that positive Q_H was indicative of the stable atmospheric conditions that are relatively common in Antarctica. It is excellent that the observations compare well with other similar observations, but the fact that the model does a poor job at simulating this important parameter is disturbing. The same study found that the turbulent fluxes supplied 36% of the energy used for surface melting on the glacier (radiation provided the other 64%). Of this, 29% was provided by the sensible heat flux and 7% by the latent heat flux. It should therefore be apparent that the model used for the Scott Base study needs to be revisited to better simulate this important feature of the surface energy balance.

Latent heat flux

As with Q_H, the model does not simulate Q_E very effectively. Unlike the observations in which negative values do occur, the model does not simulate any. The model simulates positive values for Q_E, the greatest one on day 2 reaching 1 W m^{-2}, however the observations indicate that no positive recordings were made. Other than day 2, the model simulates 0 W m^{-2} for all other time

periods. These poor results reveal themselves in the statistical analysis. The correlation coefficient is a meagre 0.1.

In 1999 (Hines *et al.*, 1999) the surface energy budget in Antarctic latitudes was evaluated for medium-range numerical weather forecasts produced by the National Centres for Environmental Prediction (NCEP) and for the NCEP - National Centre for Atmospheric Research reanalysis project during winter, spring and summer special observing periods (SOPs). The researchers found that the modelled latent heat flux was at least an order of magnitude larger than the small observations made. These larger than expected simulations of the latent heat flux are in agreement with the Scott Base case study. The authors noted that many modifications could be made to the NCEP forecasts to make results more realistic in terms of the surface energy balance. One of which was that the sensible and latent heat fluxes be reduced toward the observed values by using parameterisations appropriate for extremely stable layers. Having appropriate parameters in the model to account for stable atmospheric conditions is something that could be looked into when modelling similar conditions to the Scott Base case study in the future.

Wind direction

For wind direction, the model does quite a good job at simulating the observed results. The model agrees very well with day 1, except in the late hours of the day when the observations indicate a northwesterly and the model simulates a northeasterly. On day 2 the model simulates the general pattern but does not do a good job at simulating the extremes that the observations record, it is less variable. The model and observations are generally in good agreement for days 3 to 7. The modelled simulations tend to over estimate the value of wind directions from the northeast to southeast, by approximately 30 degrees. Other than spikes in the data where wind direction dramatically changes for a brief period of time, the model simulations wind direction quite well. This is reflected in the correlation coefficient calculated for wind direction of 0.80. The model tends to slightly overestimate all parameters that were used in statistical analysis.

Surface temperature

The simulations produced by MM5 for surface temperature agree quite well with the observed results. On days 1, 2, 6 and 7 the model underestimates the surface temperature by approximately 4°C. The model also underestimates all minimum observed temperatures,

ranging in magnitude. The model does however model the diurnal cycle of temperature very well. Individual spikes in temperature are not usually picked up by the model. As mentioned in Table 10 the statistical analysis for surface temperature is very pleasing, with a correlation coefficient of 0.89. The tendency of the model to underestimate both the maximum and minimum temperature is observed in the statistics, with the modelled minimum and maximum being a few degrees less that what is expected. This is also reflected in the mean.

Air temperature at 2 m

During the entire study period that was focussed on, the model overestimates the air temperature at 2 m for almost every data point. It also fails to register the spikes in observed temperature but does capture the diurnal fluctuation very well. The model does a particularly accurate job of simulating observations on day 6. Table 11 lists the statistical analyses performed for air temperature at 2 m. The correlation coefficient of 0.81 suggests that the model and observations correlate relatively well.

Conclusion

Observations were conducted near Scott Base during 2003-2004, with the objective of measuring parameters that may give rise to processes that control meltwater production on the McMurdo Ice Shelf. Observations were then compared with simulations produced by MM5 of the same time period, of which a portion was described in detail in this report. Some parameters such as downward shortwave radiation, upward shortwave radiation, net radiation and wind direction were accurately depicted by the modelled simulations. Others had a negative or positive bias. In this instance, the model does not capture the intensity or accuracy of the observed recordings. It is suggested that model settings be adjusted and re-run to see if more accurate simulations can be produced, especially for the turbulent heat fluxes.

Acknowledgements

The author would like to thank Dr Peyman Zawar-Reza for his expertise and supervision throughout this project. Also many thanks to Penny Clendon for the use of her observations and Mikail Titov for his modelling results.

References

Bintanja, R., 1995, "The local surface energy balance of the Ecology Glacier, King George Island, Antarctica: measurements and modelling", *Antarctic Science*, **7**(3): 315-325.

Bintanja, R., and Van Den Broeke, M.R., 1995, "The Surface Energy Balance of Antarctic Snow and Blue Ice", *Journal of Applied Meteorology*, **34**: 902-926.

Bintanja, R., and Reijmer, C.H., 2001, "Meteorological conditions over Antarctic blue-ice areas and their influence on the local surface mass balance", *Journal of Glaciology*, **47**(156): 37-50.

Guo, Z., Bromwich, D.H., and Cassano, J.J., 2003 "Evaluation of polar MM5 simulations of Antarctic atmospheric circulation", *Monthly Weather Review*, **131**(2): 384-412.

Hines, K.M., Grumbine, R.W., Bromwich, D.H., and Cullather, R.I., 1999, "Surface energy balance of the NCEP MRF and NCEP-NCAR reanalysis in Antarctic latitudes during FROST", *Weather and Forecasting*, **14**(6): 851-867.

King, J.C., 1996, "Longwave atmospheric radiation over Antarctica", *Antarctic Science*, **8**(1), 105-109.

Lewis, K.J., Fountain, A.G., and Dana, G.L., 1998, "Surface energy balance and meltwater production for a Dry Valley glacier, Taylor Valley, Antarctica.

Massachusetts Institute of Technology, 2005, "Energy Balance", retrieved 12th February 2005, from: http://web.mit.edu/globalchange/www/reports/054/node9.html

Monaghan, A.J., Bromwich, D.H., Wei, H.L., and Cayette, A.M., 2003, "Performance of weather forecast models in the rescue of Dr. Ronald Shemenski from the South Pole in April 2001", *Weather and Forecasting*, **18**(2): 142-154.

Oke, T.R., 2000, "Boundary Layer Climates, Second Edition", Routledge, London.

Orsini, A., Calzolari, F., Georgiadis, T., Levizzani, V., Nardino, M., Pirazzini, R., Rizzi, R., Sozzi, R., and Tomasi, C., 2000, "Parameterisation of surface radiation flux at an Antarctic site", *Atmospheric Research*, **54**: 245-261.

Pavolonis, M.J., Key, J.R., and Cassano, J.J., 2004, "A Study of the Antarctic Surface Energy Budget Using a Polar Regional Atmospheric Model Forced with Satellite-Derived Cloud Properties", *Monthly Weather Review*, **132**: pp 654-661.

Powers, J.G., Monaghan, J., Cayette, A.M., and Bromwich, D.H., 2003, "Real-time mesoscale modelling over Antarctica: The Antarctic Mesoscale Prediction System", *Bulletin of the American Meteorological Society*, **84**(11): 1533-1542.

Reijmer, C.H., and Oerlemans, J., 2002, "Temporal and spatial variability of the surface energy balance in Dronning Maud Land, East Antarctica", *Journal of Geophysical Research*, **107**(D24).

Trenberth, K.E., Stepaniak, D.P., and Caron, J.M., 2002, "Accuracy of atmospheric energy budgets from analyses", *Journal of Climate*, **15**(23): 3343-3361.

Turner, 1996, "The Antarctic First Regional Stud of the Troposphere (FROST) project", *Bulletin of the American Meteorological Society*, **77**: 2007-2032.

University Center for Atmospheric Research, 2005, "MM5 Modeling System Overview", retrieved 10th February 2005, from: http://www.mmm.ucar.edu/mm5/overview.html

Wendler, G., and Worbly, A.P., 2001, "The surface energy budget in Antarctic summer sea-ice pack", *Annals of Glaciology*, **33**: 275-279.